Probes of a Role for Remote Binding Interactions on Hydrogen Tunneling in the Horse Liver Alcohol Dehydrogenase Reaction†

Jodie K. Chin and Judith P. Klinman*

Departments of Chemistry and Molecular and Cell Biology, University of California, Berkeley, California, 94720

Received August 30, 1999

ABSTRACT: A tunneling contribution to hydride transfer has been demonstrated previously in the oxidation of benzyl alcohol catalyzed by an active-site mutant (F93W) of horse liver alcohol dehydrogenase (LADH) [Bahnson, B. J., et al. (1993) *Biochemistry 32*, 5503−5507]. Mutation of a residue that lies directly behind the nicotinamide ring of the bound cofactor has further shown that side-chain bulk can contribute to catalytic efficiency and tunneling in a correlated fashion [Bahnson, B. J., et al. (1997) *Proc. Natl. Acad. Sci. U.S.A. 94*, 12797−12802]. Second site mutations of F93W have now been made at positions more remote from the active site. In particular, we have focused on an isoleucine residue that interacts with the adenine moiety of the NAD^+ cofactor, 20 Å from the nicotinamide ring. Replacement of this remote residue with glycine (F93W:I224G), alanine (F93W:I224A), valine (F93W:I224V), and leucine (F93W:I224L) is concluded to destabilize the binding of NAD^+. All double mutants exhibited a K_M for NAD^+ that is 2−25 times higher than that for the F93W enzyme. However, neither the catalytic efficiency for turnover of benzyl alcohol [$k_{cat}/K_{M(benzyl\ alcohol)}$] nor the relationship between the secondary k_H/k_T and k_D/k_T isotope effects for benzyl alcohol oxidation was significantly affected. The lack of differences observed in the isotope effects indicates that these mutations have little effect on the extent of hydrogen tunneling in the reaction. The complete removal of the side chain at position 224 in the F93W:I224G enzyme resulted in a less than 5% decrease in the ratio of the secondary isotope effects, maintaining the ratio above the semiclassical limit for the indication of tunneling in the reaction. By contrast, K_i for NAD^+ increased 60-fold for this mutant. The results obtained with F93W:I224G are consistent with remote interactions that affect the association and binding of cofactor in a reactive conformation. However, once this conformation is achieved, hydride transfer and its tunneling component proceed as with the single F93W mutant enzyme, uninfluenced by the remote mutation. Replacement of other side chains, with α-carbon positions from about 8 to over 20 Å from the C4 position of the nicotinamide ring, demonstrated a similar insensitivity of $k_{cat}/K_{M(benzyl\ alcohol)}$ to protein modification. Comparison to earlier studies with active-site mutants of LADH implicates a role for proximal, but not distal, side chains in the modulation of hydrogen tunneling for this enzyme.

Enzymatic catalysis has long been thought to be facilitated by binding interactions involving substrate moieties that do not directly participate in the chemical step of the reaction (*1*). While the role of countless active-site residues has been extensively characterized in a wide variety of enzymatic systems, the significance of remote binding interactions has been less often investigated. Horse liver alcohol dehydrogenase (LADH)[1] is an excellent system for probing the role of binding interactions that are far removed from the active site of the enzyme. LADH catalyzes the transfer of hydride ion from an alcohol substrate to the NAD^+ cofactor, yielding an aldehyde and the reduced cofactor, NADH. X-ray crystallography has shown that the NAD^+ binds in an extended conformation with 15 Å between the buried, reacting carbon of the nicotinamide ring and the adenine ring near the surface of the protein (*2*). Although the second order reaction of wild-type enzyme with benzyl alcohol is partially rate-limited by aldehyde product release, it has been possible to make the chemistry more rate limiting with only a single, active-site mutation. Analysis of the relationship between the k_H/k_T and k_D/k_T isotope effects on benzyl alcohol oxidation catalyzed by the alcohol binding pocket mutant, F93W, indicated that hydrogen tunneling occurs in this reaction (*3*). The observed deviation from classical, thermally activated hydrogen transfer is expected to be highly sensitive to the height and width of the reaction barrier and, thus, should be greatly influenced by the arrangement of residues in the active site.

One of the major questions regarding the origin of nuclear tunneling in enzymatic reactions is whether this behavior is largely static, arising from properties of the potential energy surface that reflect the active-site structure of the folded protein or whether it is dependent on a dynamic component of the protein−substrate complex. As with any chemical reaction, the ground state of an enzyme-catalyzed reaction

† This work was supported by NSF Grant MCB-9514126 (J.P.K.) and NIH Molecular Biophysics Training Grant GM08295-08 (J.K.C.).

* To whom correspondence should be addressed. E-mail: klinman@socrates.berkeley.edu.

[1] Abbreviations: LADH, horse liver alcohol dehydrogenase; NAD^+, nicotinamide adenine dinucleotide; ADHht, *Bacillus stearothermophilus* alcohol dehydrogenase.

10.1021/bi9920331 CCC: $19.00
Published on Web 01/15/2000

is best considered as an ensemble of states, only some of which are competent for catalysis (*4*−*7*). This capacity to sample a range of ground-state structures may be especially critical for tunneling, given the distance dependence of such a process. Using a thermophilic alcohol dehydrogenase (ADHht) with significant homology to yeast and horse liver alcohol dehydrogenase (*4*, *8*), Kohen and Klinman (*4*) detected hydrogen tunneling at the elevated, optimal temperature of ADHht, which decreased below 30 °C. This behavior was ascribed to a rigidification of the thermophilic protein with reduced temperature, a phenomenon generally assumed (*9*, *10*) and in some instances experimentally supported (*11*−*14*) for proteins of thermophilic origin. The observation of less tunneling in the ADHht catalyzed reaction at lowered temperatures may be the result of a shift in the population of ground-state structures away from those that favor the tunneling process, or it may be due to the loss of a dynamic component(s) in the protein that facilitates the hydrogen tunneling.

In principle, both static and dynamic origins of tunneling could be enhanced by individual side chains, which are either proximal to the reacting bonds or remotely related to the active site through a network of side chains or secondary structural elements connecting the remote position to the active site. In a previous study, mutation of a bulky, hydrophobic side chain (Val203), which contacts the face of the nicotinamide ring opposite the hydrogen transfer, has been shown to decrease both the efficiency of benzyl alcohol oxidation and the tunneling contribution to hydride transfer (*15*). In the present study, we have turned to a detailed exploration of the role of a protein side chain that contacts the bound cofactor, but is removed from the active site. Studies of LADH with truncated cofactors have shown that remote contacts are important for catalysis, though their specific effect on the chemical step of the reaction has not been investigated (*16*). For example, LADH-catalyzed reaction with nicotinamide mononucleotide resulted in a 8000-fold decrease in $k_{cat}/K_{M(ethanol)}$, whereas nicotinamide hypoxanthine dinucleotide resulted in a 2.5-fold decrease. The large effect with nicotinamide mononucleotide was thought to be due to a lack of the adenosine monophosphate moiety, which is necessary for the required conformational change upon cofactor binding (*17*).

X-ray crystallography of the F93W enzyme ternary complex has shown that the cofactor NAD^+ is bound as in other LADH structures, with the adenine moiety near the surface of the protein, sandwiched between the side chains of isoleucine residues 224 and 269 (*15*). The single mutant I224G LADH was kinetically characterized by Fan and Plapp (*18*) and shown to have a decreased ability to bind cofactor, together with only a small effect on catalytic efficiency. I224G was also shown to cause changes in cofactor association and to affect the deuterium isotope effect on ethanol oxidation, with values of $^{D}V/K$ of 4.0 and ^{D}V of 1.5, as compared to wild-type values of 2.9 and 1.1, respectively. These isotope effects suggested that chemistry was more rate limiting with I224G, but more extensive measurements were required to probe the nature of hydride transfer in the reaction. Starting with F93W LADH, we have made a series of hydrophobic substitutions at position 224. The present studies indicate that tunneling and catalytic efficiency are unaltered using benzyl alcohol as a substrate, despite, in some instances, very significant changes in cofactor binding. Additional screening of mutants of LADH at other remote positions, both lining the NAD^+ binding pocket, as well as outside this cleft, has also yielded only small effects on $k_{cat}/K_{M(benzyl\ alcohol)}$.

Considering the mutants of LADH that have been characterized thus far with respect to hydrogen tunneling, an absence of a change in $k_{cat}/K_{M(benzyl\ alcohol)}$ implies that the tunneling component in the hydride transfer reaction is also likely to be unchanged. This precedent suggests that the remote mutations leading to values of $k_{cat}/K_{M(benzyl\ alcohol)}$ which are similar to wild-type are unlikely to have caused a significant change in the properties for hydride transfer. For the LADH system, we conclude that interactions at or near the reacting bonds are the key determinants in modulating hydrogen tunneling. In the context of a static view, this would imply that remote interactions are not affecting the distance for hydride transfer. Similarly, in the context of a dynamic model for tunneling, this would imply that any protein motion coupled to hydride motion is affected only by proximal residues.

MATERIALS AND METHODS

Materials. Benzyl alcohol, semicarbazide hydrochloride, pyrazole, and NAD^+ were purchased from Sigma, and 2,3,4,5,6-pentafluorobenzyl alcohol was purchased from Aldrich. Benzyl alcohol was distilled before use, and all other materials were used without further purification.

Preparation of LADH Mutants. The phagemid pBPP/LADH was used to express LADH in *Escherichia coli* XL1-Blue (Stratagene), unless otherwise noted (*19*). All mutagenic oligonucleotides were purchased from Operon Technologies, Inc. and included codon mutations as well as silent mutations to create restriction sites. All plasmid purification steps were performed with kits and materials purchased from Qiagen Inc. pBPE/*Eq*LADH containing the I224G mutation was kindly provided by Dr. Bryce V. Plapp, University of Iowa, Iowa. Construction of F93W pBPP/LADH was described previously (*3*).

For F93W:I224L, the oligonucleotide primer 5′-GG ATC ATT GGG GT**C** GAC *CTG* AAC AAA GAC-3′ was used to introduce the codon for leucine at position 224 (italicized, mutations underlined) and a silent mutation (bold) to create a *Sal*I restriction site in the F93W construct. For F93W:I224A and F93W:I224V, the primer 5′-TT GGG GT**C** GAC *NNC* AAC AAA G-3′ was used to introduce the GCC and GTC codons for alanine and valine, respectively, at position 224 and a silent mutation to create a *Sal*I restriction site in the F93W construct. F93W:K228R was constructed sequentially, starting from the wild-type LADH gene. The primer 5′-C ATC AAC AAA GAC *CGG* TTT GCA AAG GCC-3′ introduced the *CGG* codon for argenine at position 228 and the F93W mutation was incorporated as for F93W:I224G, described below. These primers were used to make mutations to the appropriate pBPP/LADH construct using the Sculptor In Vitro Mutagenesis System (Amersham). The primer 5′-GCA TTT TCC ACA **T**TG **C**GG AGT *CCA* GAG TGG GAT GAC TTT ATC ACC-3′ (noncoding) introduced the TGG codon for tryptophan at position 93 and silent mutations to create a *Bsr*DI restriction site. This primer was used with a selection primer, which changed a *Sca*I site to a *Mlu*I site

in the ampicillin resistance gene of I224G pBPE/*Eq*LADH and K228R pBPP/LADH to introduce the F93W mutation using the Chameleon Double-Stranded Site-Directed Mutagenesis Kit (Stratagene). This method was also used with the primer 5′-CCC AAT GAT CC**G** GGC CGC *TTT* GGC TGC TTT ACA GCC C-3′ (noncoding) to introduce the AAA codon for lysine at position 215 and a restriction site for *Nci*I and with the primer 5′-GAT CCT GGC CGC **G**CC GGC TGC *TNC* ACA GCC CAT-3′ (noncoding, N = G/C incorporated 50/50) to introduce the *GC*A codon for alanine at position 212 as well as an *Nae*I restriction site in the F93W construct. Expression plasmids for F93W:I269A and F93W:V294A LADH were constructed from F93W pBPP/LADH using the QuickChange Site Directed Mutagenesis Kit (Stratagene), which required a complementary set of primers. Only the coding sequence primer is given for each mutagenesis reaction. The primer 5′-GGT GTG GAT TTT TCC TTT GAA GTC *GCT* GG**A** CG**T** CTC GAC ACT ATG G-3′ introduced the GCT codon for alanine at position 269 and an *Aat*II restriction site. The primer 5′-GGT GTG ACG GTC ATT GTG GG**C** *GCG* CCT CCT GAT TCC C-3′ introduced the GCG codon for alanine at position 294, as well as a *Bss*HII restriction site.

Mutations were initially identified by restriction digest with the appropriate endonuclease and were confirmed by sequencing. DNA sequencing was performed both by using T7 Sequenase 2.0 from Amersham and by the DNA Sequencing Facility at UC Berkeley. Purification of LADH mutants was based on the procedure of Park and Plapp (*19*). Mutant proteins were purified to 95% homogeneity as determined by SDS−PAGE (*20*) and agarose gel electrophoresis (*19*, *21*).

Steady-State Kinetics. Initial velocity studies were done using a Hewlett-Packard 8452A spectrophotometer, monitoring the production of NADH at 340 nm (ϵ = 6.22 $mM^{-1}cm^{-1}$). Measurements were done at pH 7, 25 °C in 300 mM potassium phosphate and 300 mM semicarbazide-hydrochloride. The concentration of active sites was determined by spectrophotometric titration with NAD^+ in the presence of 10 mM pyrazole (*22*).

Kinetic Isotope Effects. Kinetic isotope effects were measured at pH 7, 25 °C, in 300 mM potassium phosphate, 300 mM semicarbazide−hydrochloride, and 10 mM NAD^+, using doubly labeled benzyl alcohol substrates as described, previously (*3*, *23*). Briefly, primary kinetic isotope effects were determined by comparison of the rate of tritium transfer from [1-^{3}H]benzyl alcohol or [1-^{3}H,1-^{2}H]benzyl alcohol to the rate of protium or deuterium transfer from [*ring*-^{14}C(U)]-benzyl alcohol or [1,1-$^2H_2$,*ring*-^{14}C(U)]benzyl alcohol, respectively. Secondary kinetic isotope effects were determined simultaneously by comparison of the relative reaction of substrates that were protium, deuterium, or tritium labeled on the benzylic carbon at the nontransferring hydrogen. Quenching of the reaction mixtures at 5−50% conversion was followed by quantitation of radioactivity in the substrate and products using reversed-phase HPLC and dual-label (^{3}H/^{14}C) liquid scintillation counting.

RESULTS

Mutants. Five double mutants were constructed of F93W at Ile-224: F93W:I224G, F93W:I224A, F93W:I224L, F93W:I224V, and F93W:I224F. An examination of the X-ray crystal structure of the F93W enzyme indicated that these side chains should be accommodated without obscuring the binding of cofactor. A diagram of the bound cofactor is shown in Figure 1, indicating the positions of the 93 and 224 side chains. Double mutants were also constructed of F93W at five additional sites to make F93W:I269A, F93W:K228R, F93W:G215K, F93W:K212A, and F93W:V294A (cf. Figure 1). Relative to the mutations studied previously at position 203 in the nicotinamide-binding site, all of the mutations described in this paper are more removed from the active site of the enzyme. For example, the distance between the reacting carbon of the nicotinamide ring (C4) and the α-carbon of Ile-224 is 20 Å.

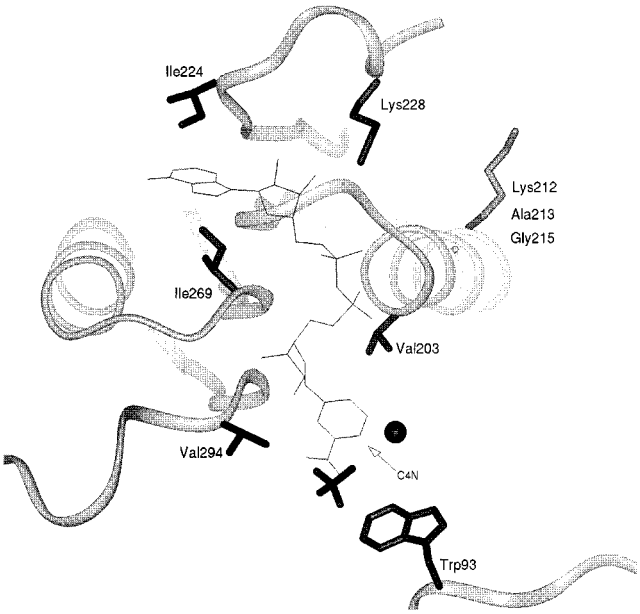

FIGURE 1: Diagram of NAD^+ bound in F93W LADH (*15*). The cofactor is shown in thin black lines and the side chains of Ile224, Trp93, Val203, Lys212, Gly215, Lys228, Ile269, and Val294 are labeled and shown in heavy black lines. The substrate analogue, trifluoroethanol is also shown in heavy black lines, near the catalytic zinc atom. The reacting carbon of NAD^+ is marked with an arrow.

Steady-State Kinetic Constants. The kinetic constants calculated from the initial rates of benzyl alcohol oxidation for F93W are compared to those for F93W:I224G, F93W:I224A, F93W:I224V, and F93W:I224L in Table 1. These parameters were determined using a fixed concentration of NAD^+ (10 mM) and varying concentrations of benzyl alcohol or a 10-fold excess over the K_M for benzyl alcohol and varying concentrations of NAD^+. Fixed concentrations of either NAD^+ or benzyl alcohol were saturating concentrations for all mutants examined. Values of k_{cat}/K_M vary by less than a factor of 2 for all of the mutants studied. The Michaelis constants for benzyl alcohol also showed little variation among the mutants. Effects of the mutations were only evident in the Michaelis constants for NAD^+, which for the mutants at Ile224 varied from about 2 to 25 times larger than for F93W LADH.

Steady-state parameters were also determined for mutant enzymes with substitutions at positions 269, 228, 215, 212, and 294, all of which are removed from the active site. There were reasons to suspect a potential role for each of these residues in catalysis. Each is conserved among most animal alcohol dehydrogenases (*24*). X-ray crystallography of the

Table 1: Kinetic Parameters and Isotope Effects for the Oxidation of Benzyl Alcohol Catalyzed by Mutants of LADH

parameter	F93W	F93W:I224A	F93W:I224L	F93W:I224G	F93W:I224V
k_{cat}/K_M (mM^{-1} s^{-1})[a]	4.6	4.3	3.4	3.0	2.7
$K_{M(benzyl\ alcohol)}$ (mM)[a]	0.07	0.1	0.2	0.3	0.1
$K_{M(NAD)}$ (mM)[a]	0.04	0.8	0.1	1.1	0.2
k_H/k_T (primary)[b]	7.61 ± 0.03 (38)	7.77 ±0.04 (21)	7.40 ± 0.05 (21)	7.51 ± 0.11 (14)	7.45 ± 0.05 (19)
k_H/k_T (secondary)[b]	1.310 ± 0.003 (38)	1.301 ± 0.005 (21)	1.289 ± 0.005 (21)	1.294 ± 0.011 (14)	1.309 ± 0.004 (19)
k_D/k_T (primary)[b]	1.85 ± 0.01 (41)	1.86 ± 0.01 (23)	1.85 ± 0.01 (19)	1.81 ± 0.01 (21)	1.81 ± 0.01 (22)
k_D/k_T (secondary)[b]	1.045 ± 0.003 (41)	1.039 ± 0.003 (21)	1.030 ± 0.003 (20)	1.045 ± 0.003 (21)	1.03 ± 0.004 (21)
$\ln(k_H/k_T)/\ln(k_D/k_T)$, primary[c]	3.29 ± 0.02	3.29 ± 0.03	3.26 ± 0.04	3.39 ± 0.04	3.39 ± 0.02
$\ln(k_H/k_T)/\ln(k_D/k_T)$, secondary[c]	6.2 ± 0.4	6.9 ± 0.6	8.6 ± 0.8	5.9 ± 0.5	9.1 ± 1.1

[a] Initial velocities were measured at pH 7, 25 °C in 300 mM potassium phosphate and 300 mM semicarbazide hydrochloride, either at varying benzyl alcohol conditions with 10 mM NAD^+ or with at varying NAD^+ concentrations with ~10 times the K_M for benzyl alcohol and were fit to the Michaelis−Menten equation using the program Kaleidagraph. Errors on steady-state parameters are less than 10% of value. [b] Reported errors are standard deviation of the mean; the number of determinations is in parentheses. [c] Errors are calculated as in Jonsson et al. (*35*).

Table 2: k_{cat}/K_M for the Oxidation of Benzyl Alcohol Catalyzed by Second Site Mutants of F93W LADH and Distances to the Active Site from the Mutated Residue[a]

mutation	k_{cat}/K_M (mM^{-1} s^{-1})	C4N.....CA (Å)[b]
V203A	0.13[c]	7.0
V294A	2.4	7.6
I269A	2.2	10.3
K228R	3.4	18.8
K212A	4.2	19.4
G215K	3.7	22.8

[a] Initial velocities were measured at pH 7 and 25 °C in 300 mM potassium phosphate and 300 mM semicarbazide hydrochloride, at varying benzyl alcohol concentrations with 10 mM NAD^+ and were fit to the Michaelis−Menten equation using the program Kaleidagraph. Errors are less than 10% of value. Distances were measured in the X-ray crystal structure of the ternary complex of F93W LADH with NAD^+ and trifluoroethanol (*15*). [b] C4N is the hydride acceptor carbon of the nicotinamide ring of NAD^+, and CA is the α-carbon for the side chain of interest. [c] Data reported previously (*15*).

Table 3: Inhibition of F93W and F93W:I224G LADH by 2,3,4,5,6-Pentafluorobenzyl Alcohol[a]

	variable substrate	inhibition	K_{is} (μM)	K_{ii} (μM)
F93W	NAD^+[b]	uncompetitive		29± 1
	benzyl alcohol[c]	competitive[f]	42 ± 4	
F93W:I224G	NAD^+[d]	uncompetitive		28 ± 2
	benzyl alcohol[e]	competitive	87 ± 7	

[a] These apparent inhibition constants were obtained from fits of initial velocities at pH 7 and 25 °C in 300 mM potassium phosphate and 300 mM semicarbazide-HCl. The concentration of inhibitor was varied from 0 to 83 μM. The data were fit to the nonlinear expressions for competitive, noncompetitive, and uncompetitive inhibition with the results from the best fit shown (*26*). [b] The concentration of benzyl alcohol was fixed at 81 μM, and the concentration of NAD^+ was varied from 35 to 518 μM. [c] The concentration of NAD^+ was fixed at 41 μM, and the concentration of benzyl alcohol was varied from 34 to 243 μM. [d] The concentration of benzyl alcohol was fixed at 0.31 mM, and the concentration of NAD^+ was varied from 0.4 to 3.2 mM. [e] The concentration of NAD^+ was fixed at 1.3 mM, and the concentration of benzyl alcohol was varied from 0.12 to 0.98 mM. [f] The data can be also be described by noncompetitive inhibition to give a K_{is} of 75 ± 14 and a K_{ii} of 139 ± 35 μM.

F93W enzyme (*15*) showed that one of the methyl groups of Val294 interacts with the "front side" of the nicotinamide ring, opposite of Val203. Val294 lies in the loop involved in the conformational change following cofactor binding, moving about 10 Å in the ternary complex as compared to the apoenzyme (*17*, *25*). Lys212 and Gly215 are at the surface exposed end of the helix that contains Val203, whose N-terminus is directed at the pyrophosphate group of the cofactor. Ile269 is the other half of the "isoleucine sandwich" around the adenine ring of the cofactor. It contacts the cofactor through main-chain interactions, as well, making a hydrogen bond to a hydroxyl group of the nicotinamide ribose ring. Last, the side chain of Lys228 hydrogen bonds to a hydroxyl group of the adenine ribose ring.

Table 2 lists k_{cat}/K_M for benzyl alcohol oxidation for these mutants and the distances between each residue and the active site of the enzyme. In contrast to the previously reported findings for position 203 (*15*), all mutants show very little effect on $k_{cat}/K_{M(benzyl\ alcohol)}$. Small effects were observed on K_M for NAD^+ and benzyl alcohol as well, with the single exception of F93W:I269A. In the latter case, K_M values of about 1 mM were observed for both substrate and cofactor.

In addition to the steady-state experiments described above, kinetic constants for F93W and F93W:I224G LADH were determined by varying the concentration of benzyl alcohol and NAD^+ and fitting the initial rates to the rate equation for a competitive ordered mechanism (*26*). The results of these experiments agreed with the data collected under pseudo-first-order conditions and allowed for a determination of the dissociation constant of the enzyme−NAD^+ complex. For F93W, K_{ia} was found to be 0.09 mM, while K_{ia} for F93W:I224G was found to be 5.7 mM. This increase of about 60-fold is comparable to that reported for the single mutant I224G enzyme as compared to wild-type LADH (*18*).

The kinetic mechanism of benzyl alcohol oxidation was also investigated more thoroughly with F93W and F93W:I224G. Dead-end inhibition studies with 2,3,4,5,6-pentafluorobenzyl alcohol yielded the kinetic constants of inhibition shown in Table 3. These data were obtained from nonlinear fits of initial velocities using the equations for competitive, noncompetitive, and uncompetitive ordered inhibition kinetics (*26*). The F93W enzyme showed uncompetitive inhibition with 2,3,4,5,6-pentafluorobenzyl alcohol against NAD^+, consistent with the mechanism that is ordered in this direction. The F93W:I224G enzyme gave similar results, and it appears from these experiments that neither the F93W nor the I224G mutation changes the overall kinetic mechanism of the benzyl alcohol oxidation reaction. 2,3,4,5,6-Pentafluorobenzyl alcohol was clearly competitive against benzyl alcohol with F93W:I224G. However, with F93W, the inhibition was not clearly competitive or noncompetitive. It is likely that the inhibitor binds to other enzyme forms, such as E·NADH, causing mixed inhibition. This is more likely to be an issue with the F93W enzyme than the F93W:I224G

enzyme, which is expected to release the reduced cofactor at an increased rate. These inhibition patterns with F93W and F93W:I224G were comparable to those observed with wild-type and the single mutant I224G using trifluoroethanol as the inhibitor (*18*).

Kinetic Isotope Effects. The nature of the hydride transfer step in the LADH catalyzed oxidation of benzyl alcohol has been studied previously by a detailed examination of primary and secondary competitive kinetic isotope effects. Solely on the basis of the difference in mass for H, D, and T, the ratio of $\ln(k_H/k_T)$ to $\ln(k_D/k_T)$ for either primary or secondary isotope effects is expected to be 3.3 (*27*). For reactions involving a moderate amount of tunneling where it is more probable that H will be transferred by tunneling than either D or T, the ratio of $\ln(k_H/k_T)$ to $\ln(k_D/k_T)$ can be much larger than 3.3 (*23*, *28*). This is the case for the F93W enzyme, where the ratio of $\ln(k_H/k_T)$ to $\ln(k_D/k_T)$ is 6.2 for the secondary isotope effects. The detection of tunneling from the deviations in the ratio of the isotope effects has been more pronounced in the secondary isotope effects in all of the mutants of LADH examined (*3*, *15*). The Ile224 mutants are not an exception to this observation, with only negligible effects in the ratios of the $\ln(k_H/k_T)$ to $\ln(k_D/k_T)$ for the primary isotope effects, which are all about 3.3, but with secondary isotope effect ratios ranging from 5.9 for F93W:I224G to 9.1 for F93W:I224V (Table 1). These secondary isotope effect ratios are not very different than that observed with F93W, and all are significantly greater than the semiclassical limit for the detection of tunneling in the reaction.

DISCUSSION

This study was conducted in the context of efforts to understand how enzymatic hydrogen tunneling is affected by the nature of interactions between a bound substrate and its cognate protein. As discussed in recent reviews (*4*, *5*), nuclear tunneling is expected to be exquisitely sensitive to both the internuclear distance between reacting atoms and the energetic relationship between bound reactant(s) and product(s). Enzymes are expected to modulate the overall barrier shape for their catalyzed reactions, and may thereby contribute to tunneling through a combination of static and dynamic factors.

Earlier investigation of a single residue that resides behind the nicotinamide ring of bound cofactor (Val203) indicated that catalytic efficiency and hydrogen tunneling are optimal when position 203 is sufficiently bulky to orient C4 of the nicotinamide ring (hydride acceptor) such that it is in close proximity to C1 of the alcohol substrate (hydride donor). Reduction in the size of residue 203 produced a regular decline in both $k_{cat}/K_{M(\text{benzyl alcohol})}$ and the signature of tunneling, $\ln(k_H/k_T)/\ln(k_D/k_T)$, Figure 2. The decrease in tunneling observed with the V203A mutation was found to be accompanied by a 0.4−0.8 Å increase in the distance between the reacting carbon atoms, as observed in the X-ray crystal structures of mutant enzyme complexes (*15*, *29*). This result is consistent with models that relate internuclear distance to tunneling efficiency and can be most simply interpreted in terms of a static role for valine 203 in modulating the reaction coordinate width. However, more recent studies of a thermophilic alcohol dehydrogenase, ADHht, which is homologous to LADH, indicate that protein flexibility plays a critical role in supporting nuclear tunneling in an enzyme-catalyzed reaction. The influence of a protein vibration on hydrogen transfer has been modeled, for example, by Schwartz and co-workers (*30*), who propose that coupling of a protein normal mode to the hydrogen transfer reaction coordinate may substantially increase the rate for hydrogen transfer. In this model, side-chain interactions with substrates or within the protein itself could participate in the protein mode that is coupled to the reaction coordinate.

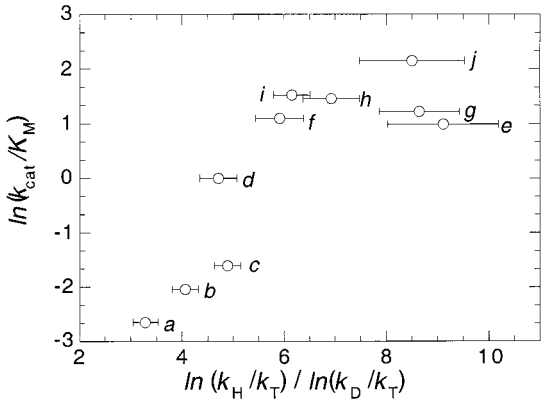

FIGURE 2: Correlation between the $\ln(k_{cat}/K_M)$ and the ratio of $\ln(k_H/k_T)/\ln(k_D/k_T)$ for the secondary isotope effects observed with site directed mutants of alcohol dehydrogenase [points a−d reported previously (*15*)]. Point a, V203G; point b, F93W:V203A; point c, V203A; point d, V203L; point e, F93W:I224V; point f, F93W:I224G; point g, F93W:I224L; point h, F93W:I224A; point i, F93W; point j, L57F.

It has long been recognized that proteins use binding interactions to facilitate catalysis. These binding interactions may lie close to the reacting bonds or may be quite far away in the case of large, extended cofactors. The LADH studies carried out with mutants of Val203 demonstrate the role of a proximal active site binding interaction (*15*, *29*). LADH is an ideal system in which to gauge the role of remote binding interactions, due to the extended conformation of the bound cofactor and the well documented role for hydrogen tunneling in substrate oxidation. The high sensitivity of tunneling to reaction barrier shape allows a unique assessment of the role of side-chain interactions in the LADH-catalyzed reaction. The present study describes an in depth investigation of the effect of a series of side-chain alterations at position 224. Additionally, other residues that are remote from the reaction center have been examined (Figure 1).

Residue 224 is of particular interest because of its large distance from the reacting carbons in the active site, together with its direct interaction with a portion of the bound cofactor. X-ray crystal structures and structures inferred from sequence alignments for both alcohol dehydrogenases and other NAD^+ binding proteins (*24*, *31*) indicate a hydrophobic residue at a position analogous to 224 in LADH; adenylate-binding protein motifs contain this hydrophobic residue, as well (*32*). Earlier studies by Plapp and co-workers (*18*) had shown that mutation of Ile224 led to a relatively small effect on the magnitude of $k_{cat}/K_{M(\text{ethanol})}$. This effect on catalysis contrasted with a 30-fold decrease in the rate of association of NAD^+ and a 200-fold increase in $K_{M(NAD)}$ as compared to wild-type enzyme, which is unexpected in the context of

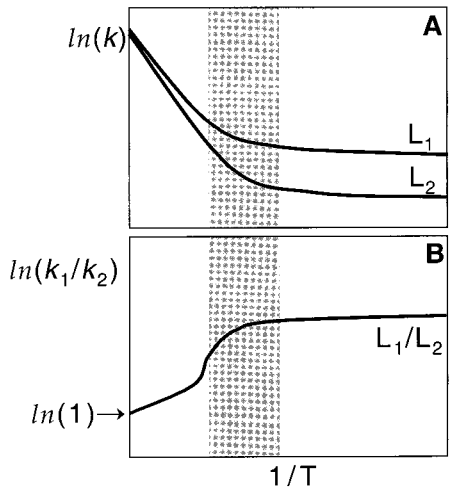

FIGURE 3: (A) An Arrhenius plot of rate, ln(k), against 1/T (temp, K), for a light isotope (L_1, i.e., H) and a heavier isotope (L_2, i.e., D). The region of interest, where the curvature for L_1 and L_2 is high, is shaded. (B) An Arrhenius plot of the isotope effect, ln(k_1/k_2) against 1/T. The corresponding region of interest is shaded, showing that in this region of little change in rate, there is an appreciable change in the isotope effect.

models that involve a role for remote binding interactions in catalysis.

Analyses of hydrogen tunneling in systems different from LADH have indicated the possibility of structural effects that lead to little or no change in k_{cat}/K_M for protiated substrate, together with sizable effects on the degree of tunneling. This can be understood in the context of comparative Arrhenius plots for a light and heavy isotope, which demonstrate a transition from moderate to extensive tunneling (gray region of Figure 3). Such a transition produces curvature in Arrhenius plots such that the rate may change relatively little with temperature. By contrast, since the temperature region for curvature is isotope dependent, the temperature dependence of the isotope effects shows anomalies, and extrapolates to isotope effects on Arrhenius prefactors that can be greater or less than the semiclassical limit of unity. Behavior of this nature has been reported for glucose oxidase (*33*) and, more recently, observed in a mutant form of lipoxygenase that shows little change in k_{cat} together with a very different temperature dependence of the isotope effects than seen with wild-type enzyme (K. Rickert and J. Klinman, unpublished results).

For this reason, we made the decision to explore the relationship between ln(k_H/k_T) and ln(k_D/k_T) for mutants of LADH that contain side chains of varying size and hydrophobicity at position 224. This comparison of ln(k_H/k_T) to ln(k_D/k_T) as a probe for tunneling is preferable to the study of temperature-dependent isotope effects because of the increasing importance of kinetic complexity at temperatures different from 25 °C in the LADH reaction.

The results in Table 1 indicate that position 224 can tolerate quite drastic alterations without substantial effects on ln(k_H/k_T)/ln(k_D/k_T). Within experimental error, there are only very small differences in the signature of tunneling for the mutants, leading to the conclusion that tunneling in LADH is essentially unaffected by the side chain at position 224. This failure to see any indication of a change in tunneling when $k_{cat}/K_{M(benzyl\ alcohol)}$ is unaltered is consistent with earlier conclusions of only moderate tunneling in both yeast and horse liver alcohol dehydrogenase at 25 °C (*3*, *15*, *23*). Such behavior would place LADH to the left of the gray area in Figure 3.

Scheme 1

$$E + NAD^+ \overset{K_1}{\rightleftharpoons} E{\bullet}NAD^+ \overset{K_2}{\rightleftharpoons} E'{\bullet}NAD^+$$

The data at position 224 serve as a control for previously published data for a mutant of LADH at position 203 (Figure 2). They also suggest that mutant forms of LADH with unaltered values for $k_{cat}/K_{M(benzyl\ alcohol)}$ will retain their tunneling capacity. The screening of a series of remote positions for the effects of side-chain modification was, therefore, pursued by investigation of rate alone. The residues examined are highlighted in Figure 1 and the results are summarized in Table 2. While the choice of residues was complicated, given the large number from which to chose, there was a rationale for studying each of them, as discussed in the Results. *Quite remarkably, not a single residue outside the nicotinamide-binding site has been found to have a demonstrated effect on catalytic efficiency in LADH, despite measurable changes in the K_M for cofactor.*

Two questions remain to be addressed. First, with regard to position 224, why is the Michaelis constant for NAD^+ increased without an accompanying effect on the efficiency of hydrogen tunneling? This can be most simply understood in the context of coupled equilibria (Scheme 1), in which the capacity of NAD^+ to bring about a well-documented, catalytically essential conformational change is compromised for mutant proteins. In the context of the present studies, we conclude that once the concentration of NAD^+ is high enough to drive enzyme toward E′•NAD^+, tunneling proceeds as for wild-type.

The second question of great interest is why Val203 is the only residue that has been shown to produce a change in both catalytic efficiency and tunneling. Clearly, the data amassed thus far argue for a proximal, but not a distal, effect in the modulation of hydrogen transfer efficiency. This may be understood by considering the computational work of Bruice and co-workers (*34*), who argue that the nicotinamide ring assumes a quasi-boat conformation during catalysis. The bulky, hydrophobic residue behind C4 of the nicotinamide ring is expected to influence such a conformational change. Interestingly, theoretical studies done by Schwartz and coworkers have shown that mathematical coupling of a protein mode to the reaction coordinate could increase the hydrogen transfer rate, substantially (*30*). Close proximity would be a prerequisite for any interacting vibrations, and it is possible that only nearby residues would participate in these modes. However, we note that the X-ray crystal structure characterization of both V203A and F93W:V203A LADH indicate an increase in the distance between C4 of bound cofactor and C1 of substrate (*15*, *29*). This suggests that a simple change in barrier width may be the dominant feature controlling tunneling efficiency in LADH. For the future, biophysical studies appear to be essential, which will permit a direct analysis of dynamical features of both wild-type and mutant forms of protein. In this way, it may be possible to document changes in the dynamical features of a protein structure that accompany changes in reaction properties and tunneling.

REFERENCES

1. Jencks, W. P. (1975) *Adv. Enzymol. 43*, 219−410.
2. Ramaswamy, S., Eklund, H., and Plapp, B. V. (1994) *Biochemistry 33*, 5230−5237.
3. Bahnson, B. J., Park, D. H., Kim, K., Plapp, B. V., and Klinman, J. P. (1993) *Biochemistry 32*, 5503−5507.
4. Kohen, A., and Klinman, J. P. (1999) *Chem. Biol.* (in press).
5. Kohen, A., and Klinman, J. P. (1998) *Acc. Chem. Res. 31*, 397−404.
6. Cannon, W. R., Singleton, S. F., and Benkovic, S. J. (1996) *Nat. Struct. Biol. 3*, 821−833.
7. Austin, R. H., Beeson, K. W., Eisenstein, L., Frauenfelder, H., and Gunsalus, I. C. (1975) *Biochemistry 14*, 5355−5373.
8. Cannio, R., Rossi, M., and Bartolucci, S. (1994) *Eur. J. Biochem. 222*, 345−352.
9. Jaenicke, R. (1991) *Eur. J. Biochem. 202*, 715−728.
10. Somero, G. N. (1995) *Annu. Rev. Physiol. 57*, 43−68.
11. Lakatos, S., Halász, G., and Závodszky, P. (1978) *Biochem. Soc. Trans. 6*, 1195−1197.
12. Závodszky, P., Kardos, J., Svingor, and Petsko, G. A. (1998) *Proc. Natl. Acad. Sci. U.S.A. 95*, 7406−7411.
13. Varley, P. G., and Pain, R. H. (1991) *J. Mol. Biol. 220*, 531−538.
14. Wrba, A., Schweiger, A., Schultes, V., Jaenicke, R., and Závodsky, P. (1990) *Biochemistry 29*, 7584−7592.
15. Bahnson, B. J., Colby, T. D., Chin, J. K., Goldstein, B. M., and Klinman, J. P. (1997) *Proc. Natl. Acad. Sci. U.S.A. 94*, 12797−12802.
16. Plapp, B. V., Sogin, D. C., Dworschack, R. T., Bohlken, D. P., Woenckhaus, C., and Jeck, R. (1986) *Biochemistry 25*, 5396−5402.
17. Eklund, H., Samama, J. P., and Jones, T. A. (1984) *Biochemistry 23*, 5982−5996.
18. Fan, F., and Plapp, B. V. (1995) *Biochemistry 34*, 4709−4713.
19. Park, D. H., and Plapp, B. V. (1991) *J. Biol. Chem. 266*, 13296−13302.
20. Laemmli, U. K. (1970) *Nature 227*, 680−685.
21. Manchenko, G. P. (1994) *Handbook of Detection of Enzymes on Electrophoretic Gels*, CRC Press, Boca Raton.
22. Theorell, H., and Yonetani, T. (1963) *Biochem. Z. 338*, 537−553.
23. Cha, Y., Murray, C. J., and Klinman, J. P. (1989) *Science 243*, 1325−1330.
24. Sun, H.-W., and Plapp, B. V. (1992) *J. Mol. Evol. 34*, 522−535.
25. Colonna-Cesari, F., Perahia, D., Karplus, M., Eklund, H., Brändén, C. I., and Tapia, O. (1986) *J. Biol. Chem. 261*, 15273−15280.
26. Cleland, W. W. (1967) *Adv. Enzymol. 29*, 1−32.
27. Swain, C. G., Stivers, E. C., Reuwer, J. F., Jr., and Schaad, L. J. (1958) *J. Am. Chem. Soc. 80*, 5885−5893.
28. Saunders, W. H., Jr. (1985) *J. Am. Chem. Soc. 107*, 164−169.
29. Colby, T. D., Bahnson, B. J., Chin, J. K., Klinman, J. P., and Goldstein, B. M. (1998) *Biochemistry 37*, 9295−9304.
30. Antoniou, D., and Schwartz, S. D. (1997) *Proc. Natl. Acad. Sci. U.S.A. 94*, 12360−12365.
31. Rossmann, M. G., Moras, D., and Olsen, K. W. (1974) *Nature 250*, 194−199.
32. Moodie, S. L., Mitchell, J. B. O., and Thornton, J. M. (1996) *J. Mol. Biol. 263*, 486−500.
33. Kohen, A., Jonsson, T., and Klinman, J. P. (1997) *Biochemistry 36*, 6854−6854.
34. Bruice, T. C., and Lightstone, F. C. (1999) *Acc. Chem. Res. 32*, 127−136.
35. Jonsson, T., Edmondson, D. E., and Klinman, J. P. (1994) *Biochemistry 33*, 14871−14878.

BI9920331